JCTC Journal of Chemical Theory and Computation

Can Range-Separated and Hybrid DFT Functionals Predict Low-Lying Excitations? A Tookad Case Study

Boxue Tian,[†] Emma S. E. Eriksson,[†] and Leif A. Eriksson*[,†,‡]

School of Chemistry, National University of Ireland - Galway, Galway, Ireland and Örebro Life Science Center, School of Science and Technology, Örebro University, 701 82 Örebro, Sweden

Abstract: The spectral properties of Tookad (Pd-bacteriopheophorbide, Pd-BPheid), an effective photosensitizer that targets mainly prostate tumors, and metal-free BPheid have been studied using time-dependent density functional theory (TD-DFT). The well-established B3LYP functional, which is known to overestimate excitation energies, was included in the study along with recently introduced range-separated and meta hybrid DFT functionals CAM-B3LYP, M06, M06-2X, M06HF, ωB97XD, ωB97X, ωB97, LC-ωPBE, and PBE0 (PBE1PBE). The main focus is the performance of the new functionals in predicting low-lying excitations (>600 nm), to explore their potential roles in drug development for photodynamic therapy. The data suggests that ωB97XD overall performs best for the Q_y transition band (the red-most absorption), followed by CAM-B3LYP. LC-ωPBE, ωB97, B3LYP, and PBE1PBE all generated the Q_y band far from the experimental position. The error in absorption energy for the Q_y band was found to be at most 0.05 eV for ωB97XD, compared to 0.15−0.19 eV for B3LYP. The use of different basis sets used in excited-state calculations was shown to be of less importance as was the use of either B3LYP or M06 in geometry optimizations.

1. Introduction

Photodynamic therapy (PDT), in which a photosensitizer, light, and oxygen are the major components, has been shown to be a promising method for treatment of various cancers as well as other diseases. In the reaction between the excited photosensitizer and oxygen in the tissue, reactive oxygen species (ROS), such as singlet oxygen, are formed and can readily react with the target tissue. Photosensitizers are light-absorbing molecules often made up by conjugated systems, such as porphyrins, chlorins (17,18-dihydroporphyrin), and bacteriochlorins (7,8,17,18-tetrahydroporphyrin). The first approved and most widely used photosensitizer is Photofrin that has been successfully used in PDT. However, Photofrin suffers from drawbacks, such as light absorption at wavelengths below the optimal tissue penetration as well as long-lasting photosensitization, due to accumulation in the skin

tissue (low-clearance rate). Additional photosensitizers are now available on the market, and new photosensitizers are continuously being developed with the aim to reduce the side effects and increase the efficiency of the treatment.

One of the most important aspects in the development of photosensitizers is the absorption properties. The red-most absorption peak of porphyrin- and chlorin-based photosensitizers is in general positioned between 600 and 700 nm and is the one used in PDT to excite the photosensitizer. Although this is usually significantly weaker than absorptions occurring around 400 nm, it is used in PDT due to the increased tissue penetration of the light at these wavelengths. Bacteriochlorophylls (BChl) display relatively speaking very large extinction coefficients for the low-lying Q_y band, and thus some BChls and their derivatives have been suggested to be utilized as photosensitizers in PDT.[1,2] Substitution of the central Mg^{2+} in native BChl with other divalent transition-metal ions, such as Pd^{2+}, Co^{2+}, Ni^{2+}, Cu^{2+}, Zn^{2+}, and Mn^{2+} has been carried out successfully,[3] and the spectroscopic properties of these synthesized compounds

* Corresponding author. E-mail: leif.eriksson@nuigalway.ie.
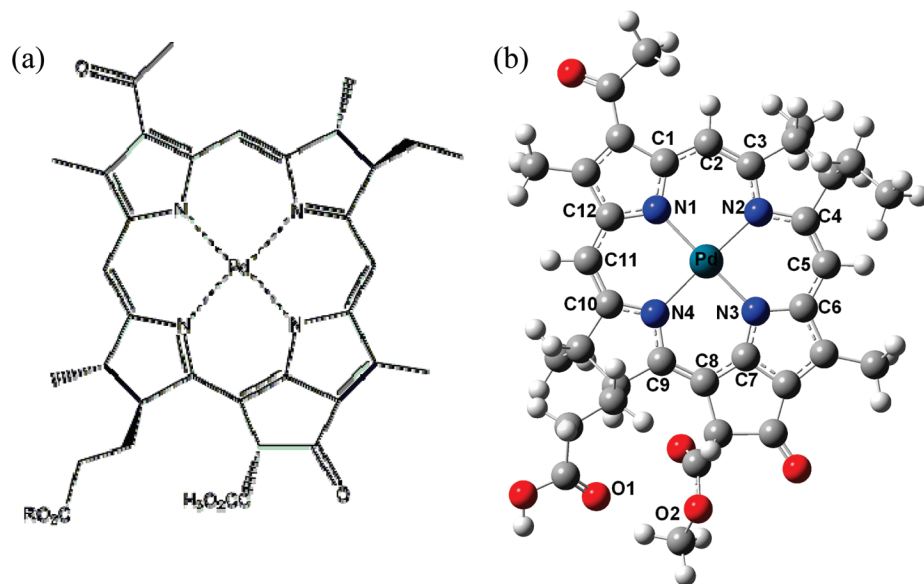† National University of Ireland.
‡ Örebro University.

Figure 1. (a) Schematic figure of the Tookad molecule. R = H: Tookad (Pd-BPheid); R = $C_{20}H_{39}$: Pd-BChl. (b) Optimized structure of the Tookad molecule.

have been extensively studied. BChl with the central metal removed and replaced by two hydrogen atoms (bacteriopheophytin, BPhe) displays its two red-most absorption peaks at 749−758 and at 524−531 nm in diethyl ether (DE),[3−5] toluene, and tetrahydrofuran (THF),[4] corresponding to the Q_y and Q_x transition bands, respectively. Metal-containing BChls absorb strongly at wavelengths in the range of 753−782 nm, and the second absorption peak is observed at 529−594 nm in DE and THF.[3,6] From these data, it is clear that the change of metal in the molecular center significantly affects the position of the Q_x band, whereas the position of the low-lying Q_y band is less dependent on the metal.

Pd-containing BChl derivatives have achieved particular attention due to enhanced stability and promising photodynamic properties. Tookad (WST09), displayed in Figure 1, is a Pd-containing BChl derivative in which the phytyl group ($C_{20}H_{39}$) at the propionyl residue has been replaced by a hydrogen atom, giving Pd-bacteriopheophorbide (Pd-BPheid). However, the presence or absence of the phytyl group does not affect the position of the absorption bands as the phytyl group does not contribute to the conjugation,[7,8] and spectroscopic data reported for Pd-BChl and Tookad are therefore almost identical. Pd-BChl displays the Q_y and Q_x absorption bands at 753−762 nm and 527−535 nm in DE,[3,5] toluene,[9] and THF.[6] For Pd-BChl and Tookad, the quantum yield for intersystem crossing from the first-excited singlet state to the triplet state is nearly 100%, which results in a large number of triplet-state molecules available to react with molecular oxygen, with the main product being singlet oxygen.[9,10]

In vitro and in vivo studies on the effect of Tookad-PDT have showed significant phototoxicity on several different carcinoma cells and tumors as a result of tumor vascular damage.[11−17] The promising results from these studies have led to phase I[18−20] and II[21] clinical trials performed on patients with prostate cancer. Tookad has, as opposed to several other photosensitizers, a fast clearance rate from the body.[22] It does not seem to accumulate in skin, muscle, and tumor tissue but mainly in the plasma, kidney, and liver, from which it is cleared relatively rapidly.[22] The low accumulation in skin tissue would reduce the long-lasting photosensitization side effects common for photosensitizers, such as Photofrin.

Computational modeling holds good promise for drug development and refinement, in that we are able to process large quantities of data in a short period of time and thus point to modifications (or entirely new molecules) that would be of interest to synthesize and assess experimentally. In the current context, if we are to find improved chromophores for PDT, then the capability to compute accurate absorption spectra would be essential for the methodology chosen. As the molecules discussed herein are rather large, and it would be desirable to explore changes in spectra for a significant number of possible substitutions, excited-state calculations within the time-dependent density functional theory (TD-DFT) formalism is an attractive option.

TD-DFT has been employed successfully over the past decade to explore both spectra and photochemical properties on a wide range of systems. However, an early comparative study of the performance of TD-DFT versus CASSCF/CASPT2 (multiconfigurational SCF and second-order perturbation theory) on excited-state calculations of a number of organic compounds showed that the methodology suffers from defects that makes it less accurate compared with pure ab initio methods.[23] Several benchmarking studies of excited-state calculations using more recent DFT functionals have since been reported. Perpète et al used B3LYP and PBE0 to explore absorptions of 66 different substituted anthraquinones, showing that PBE0 was able to provide data to within a mean average deviation (MAD) of 0.05 eV after the application of a fitting procedure for this particular set of systems.[24] Andzelm et al used eight different functionals (including HF and local density functionals) for a set of tricyanofuran based push−pull (donor−acceptor) chromophores.[25] Again the PBE0 functional, along with CAM-

B3LYP and BNL, were found to perform the best after adjustment of the attenuation factor γ. However, the data showed large spread, and issues, such as transferrability and uneven performance for charge-transfer versus $\pi-\pi^*$ excitations, remain to be resolved. Two larger functional benchmark studies have been reported by Jacquemin et al, dealing with singlet excited states and singlet−triplet gaps, respectively.[26,27] In their extensive study of singlet excitations, 29 functionals were tested, computing 700 excitations for 500 organic molecules of varying sizes.[26] The data show a very large system dependence, with the best MAD of about 0.25 eV. Functionals containing a large fraction of exchange significantly underestimated the excitation energies, and overall the functionals of 'standard hybrid' type, such as X3LYP, B3LYP and PBE0, performed the best. In the study of singlet−triplet gaps, finally, 34 functionals were included to study a total of 63 excited states in 20 medium-sized molecules.[27] Again, the functionals displayed a large spread, with functionals both over- and under-shooting; the MAD varying between 0.2−0.7 eV. The BMK and M06-2X functionals were in this case found to perform the best, albeit M06-2X is unpredictable in that it sometimes gives too high and sometimes too low values; PBE0 and CAM-B3LYP were also among the better-performing functionals but consistently overshot the experimental excitation energies.

A large number of computational studies on photosensitizing compounds based on porphyrin, chlorin, and bacteriochlorin structures have also been reported. As in the benchmarking examples outlined above, excited-state calculations have been performed using different methods, generating deviating results. Palma et al. recently summarized the present computational results on free-base porphyrin and chlorin obtained by different methods and functionals.[28] It is clear from these data that TD-DFT in combination with any functional used in those studies overestimates the excitation energy of the Q_y band by 0.11−0.34 eV. Excited-state calculations of metal-coordinated porphyrins, e.g. Zn−porphyrin,[29,30] performed at the TD-DFT/B3LYP level of theory, also overestimated the excitation energies.

A four-orbital model has been suggested in order to explain the four transitions (two Q and two B bands) seen in the absorption spectra of porphyrins.[31] This model only considers the two highest occupied molecular orbitals (HOMO-1 and HOMO) and the two lowest unoccupied molecular orbitals (LUMO and LUMO+1) and the four possible excitations between those. However, the four-orbital model has been questioned as both experimentally and theoretically more than four transition bands have been found. Still the question is being discussed as diverging results are being generated, and different conclusions are drawn. In the case of more than four transition bands found the result can be interpreted either as if the additional bands found represent vibrational overtones of the electronic transition bands,[32] hence the four-orbital theory would hold, or as if all observed bands are electronic transitions,[33] meaning that the four-orbital model would be inappropriate. Recent theoretical studies performed on chlorophyll a and pheophytin a have not thrown further light on the issue. Symmetry-adapted cluster configuration interaction (SAC−CI) calculations[34] support the four-orbital

model by generating only four transition bands, in agreement with the ones found by Houssier et al.[32] At the TD-DFT/Becke−Perdew (TD-DFT/B-P)[7,8] and DFT with multireference configuration interaction (DFT/MRCI)[35] level of theory however, apart from the four transition bands, additional bands are found in-between the Q bands as well as at higher energies, results that support the assumption that the four-orbital model is too simple to correctly describe the absorption spectra.[33] From these studies it is also concluded that TD-DFT overestimates the excitation energy of the Q_y band.

In order to try to establish a suitable methodology for the study of these types of systems, we have in the present study investigated Tookad and metal-free BPheid with the aim to assess the performance of nine recent functionals in predicting low-lying excited-state energies, i.e., evaluating their predictive power and hence potential to use in computer-assisted drug design for PDT. The main question to be answered is if either of these functionals can reproduce the long wavelength peak of the absorption spectrum, a task in which several commonly applied functionals today fail. We used B3LYP,[36] PBE0[37] (PBE1PBE), LC-ωPBE,[38−41] CAM-B3LYP,[42] ωB97,[43] ωB97X,[43] ωB97XD[44], M06,[45] M06-2X,[45] and M06HF[46,47] for excited-state calculations and B3LYP and M06 for geometry optimizations. In order to explore if the presence or absence of a metal in the compound affects the performance of the functionals, both Tookad (Pd-BPheid) and metal-free BPheid were included.

LC-ωPBE, CAM-B3LYP, and ωB97XD are so-called long-range corrected (LC) functionals in which the Coulomb r_{12}^{-1} term is split into a long-range part that includes the Hartree−Fock (HF) exchange integral and a short-range part that includes the DFT exchange interaction. The ω parameter is introduced to control the range of the interelectronic separation between the two terms. LC-ωPBE is the long-range corrected version of the nonempirical generalized gradient approximation (GGA) functional ωPBE (Perdew−Burke−Ernzerhof). CAM-B3LYP uses a Coulomb attenuating method to combine the hybrid B3LYP method with a long-range correction by introducing two extra parameters, instead of the single parameter used by Becke. ωB97XD is an extended version of the long-range corrected ωB97 and ωB97X functionals with empirical dispersion correction. M06HF is a full-HF exchange functional with satisfying long-range properties, primarily designed for Rydberg and charge-transfer excitations. M06 and M06-2X, finally, are a extensions of M06HF, with focus on valence excitations.

2. Computational Methodology

All calculations were carried out using the Gaussian09 program.[48] Neutral Tookad and the corresponding metal-free BPheid were studied. The geometries of the ground singlet state of the molecules were initially optimized in vacuum, toluene, and THF using B3LYP and M06. The LanL2DZ[49] basis set, an effective core potential (ECP) and valence electron (double-ζ) basis set combination, was used for Pd, and the 6-31+G(d,p) all-electron basis set was used for all other atoms in the geometry optimizations. The bulk solvation was modeled through the integral equation formalism of the polarized continuum model (IEF-PCM).[50,51]

A Tookad Case Study

J. Chem. Theory Comput., Vol. 6, No. 7, 2010 **2089**

Table 1. Selected Geometrical Parameters for Tookad Optimized in Toluene with B3LYP and M06 in Conjunction with LanL2DZ Basis Set for Pd and 6-31+G(d,p) for All Other Atoms[a]

	distance (Å)	
atoms	B3LYP	M06
Pd−N1	2.054	2.048
Pd−N2	2.062	2.050
Pd−N3	2.015	2.010
Pd−N4	2.114	2.100
(N1···N3)	4.069	4.058
(N2···N4)	4.175	4.149
N1−C1	1.367	1.362
C1−C2	1.400	1.396
C2−C3	1.395	1.381
C3−N2	1.357	1.351
N2−C4	1.379	1.376
C4−C5	1.377	1.373
C5−C6	1.406	1.403
C6−N3	1.384	1.378
N3−C7	1.337	1.332
C7−C8	1.399	1.395
C8−C9	1.377	1.372
C9−N4	1.381	1.375
N4−C10	1.359	1.353
C10−C11	1.384	1.381
C11−C12	1.398	1.393
C12−N1	1.371	1.366
(O1···O2)	3.499	3.142

[a] Atom names correspond to the labels in Figure 1b.

Vertical singlet excitation energies were calculated in vacuum, toluene, and THF for Tookad and BPheid using both structures optimized with B3LYP and M06, employing the time-dependent (TD) formalism[52−54] and the B3LYP, M06HF, and ωB97XD functionals. For the Tookad and BPheid geometries optimized using B3LYP, vertical singlet excitation energies in toluene were also calculated using CAM-B3LYP, M06, M06-2X, ωB97X, ωB97, LC-ωPBE, and PBE0. The LanL2DZ and 6-311+G(2d,2p) basis sets were used in the excited-state calculations. The basis sets 6-31G(d,p) and 6-31+G(d,p) (for all atoms but Pd) were also included in a test set of excited-state calculations with ωB97XD on the Tookad B3LYP geometry in toluene. The calculated wavelengths (in nm) are plotted against the oscillator strengths using a Gaussian line shape.

3. Results

3.1. Geometry. First the effect on the optimized geometries by the two different functionals was investigated. This is an important aspect to consider as geometrical changes can greatly influence the excitation properties of the molecule. Selected geometrical parameters for Tookad optimized in toluene using B3LYP and M06 are shown in Table 1, and Cartesian coordinates are provided in the Supporting Information. The data show that M06 generates a structure with an overall more 'compact' conjugated core.

The tail parts of the molecule (represented by the O1···O2 distance in Table 1 and Figure 1) are most affected by the choice of functional and can, without explicitly taking part in the conjugation, influence the conjugated system by affecting the geometry of the ring system. However, the small differences in lengths for the bonds participating in the

Table 2. Calculated Low-Lying Absorption Bands (Q_y and Q_x) for Tookad (Pd-BPheid) and BPheid in Toluene and THF[a]

		solvent = toluene		solvent = THF	
geometry	TD-DFT	Q_y	Q_x	Q_y	Q_x
		Tookad			
	Exptl[9]	762	535	Exptl[6] 755	529
B3LYP	B3LYP	695	528	693	530
	M06HF	810	523	743	521
	ωB97XD	769	528	750	527
M06	B3LYP	690	524	688	526
	M06HF	805	519	745	517
	ωB97XD	763	523	746	522
		BPheid			
	Exptl[4]	758	531	Exptl[4] 751	527
B3LYP	B3LYP	681	554	679	554
	M06HF	777	530	708	524
	ωB97XD	759	553	738	550
M06	B3LYP	679	549	678	549
	M06HF	760	524	689	517
	ωB97XD	753	547	729	544

[a] Compared with experimental data for Pd-BChl and BPhe.

conjugated system have only a minor effect on the calculated spectra, as shown below.

The effect of the environment (gas phase, toluene, and THF) on the geometries is also mainly seen in the two tails of the molecule (data shown for toluene only, Table 1). The metal has a small effect on the geometry of the molecule. The presence of Pd in the structure attracts the nitrogen atoms in a way that the inner core of the ring system becomes more compact (atom distances N1···N3 and N2···N4 are reduced) compared to the metal-free system (data not shown).

3.2. Spectroscopic Properties. Table 2 shows the calculated lowest-lying absorption bands for Tookad and BPheid in toluene and THF, along with the experimental data for Pd-BChl and BPhe. As previously mentioned, the spectral properties should not be affected to any significant degree by the presence or absence of the phytyl group. The functionals B3LYP and M06 were used together with the LanL2DZ and 6-31+G(d,p) basis sets in the geometry optimizations, and B3LYP, M06HF, and ωB97XD in conjunction with the LanL2DZ and 6-311+G(2d,2p) basis sets were used in the excited-state calculations. Only the two red-most absorption bands (Q_x and Q_y) are discussed here, as the complete experimental spectra are not available for the compounds in both solutions. In addition, the Q_x and Q_y bands correspond to the absorption wavelengths of interest when studying properties related to PDT.

Excited-state calculations using the same functional (B3LYP, M06HF, or ωB97XD) on the B3LYP or M06 geometries generate absorption bands in the same range, within 2−6 and 1−19 nm for Tookad and BPheid, respectively. The M06 geometry results overall in slightly shorter wavelengths compared with the B3LYP geometry, however the difference is not significant.

The choice of functional used for excited-state calculations is more crucial, and the different functionals generate quite

widespread results. Excited-state calculations using B3LYP overall generates the Q_y band at shorter wavelengths than ωB97XD, whereas M06HF generates the Q_y band at longer or shorter wavelengths, depending on solvent. The choice of functional thus significantly affects the position of Q_y band, whereas the Q_x band is almost independent of the functional used. It is well-known that B3LYP in general overestimates excitation energies by ∼0.1−0.2 eV, however when there is charge transfer involved the error should be larger. It is clear also from the results presented herein that the energies of the first excitation are overestimated using B3LYP. For Tookad, the excitation energy of the Q_y band is overestimated by 0.15−0.17 eV, whereas for BPheid the energy difference is slightly larger, 0.18−0.19 eV. For M06HF and ωB97XD, the results are inconsistent; in some cases, the excitation energies are either underestimated or overestimated, but overall, the results are closer to the experimental data than B3LYP. For M06HF, the error is in the range of 0.02−0.10 and 0−0.15 eV for Tookad and BPheid, respectively, and for ωB97XD, the error range is 0−0.02 and 0−0.05 eV for Tookad and BPheid, respectively. The error of the Q_x band is overall significantly smaller than for the Q_y band. It cannot be concluded from the generated results if the presence of the metal significantly influences the performance of the functionals. The solvent only affects the absorption peaks a few nm for B3LYP and ωB97XD, which is consistent with experimental data, whereas for M06HF the difference between the two solvents is significant for the Q_y band.

For Tookad, it is obvious that ωB97XD used in excited-state calculations generates absorption wavelengths closest to the experimental ones for the Q_y band. For the Q_x band, the performance of the functionals is more inconsistent; however, the difference between the functionals is small. ωB97XD and B3LYP generate results closest to experimental data in this case. For BPheid, ωB97XD again generates the best result for the Q_y band in three cases out of four. For the Q_x band, however, the functionals do not perform as equally as for Tookad, and the results show that M06HF generates the best result. However, for the Q_y band of both Tookad and BPheid, M06HF generates results far from experimental data in several cases. Gas-phase data are included in the Supporting Information. The absorption bands generated with B3LYP and ωB97XD in the gas phase are all blue-shifted compared with in bulk solvation. For M06HF, however, the Q_y band is in some cases not affected at all by the inclusion of bulk solvation, and the gas-phase data is also sometimes red-shifted compared with the data in bulk solvation. The Q_y band is most affected by the inclusion of bulk solvation, whereas the Q_x band is only red-shifted a few nm. These results confirm that including implicit solvent is in general necessary in order to obtain reasonable data.

In order to display the effect of the Pd atom on the absorption spectra, a comparison between Tookad and metal-free BPheid is displayed in Figure 2. Here we display the case in which ωB97XD was used for excited-state calculations in toluene on the B3LYP geometries. BPheid displays a more compressed spectrum, with the Q_y band blue-shifted, i.e., more energy is needed to excite BPheid to its first excited singlet state, compared with Tookad. The high-energy region
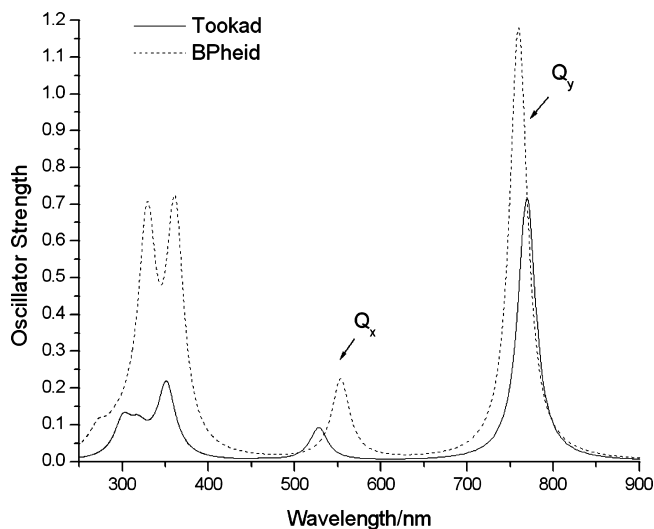

Figure 2. Absorption spectra of Tookad and BPheid generated using ωB97XD.

of the spectra is similar for the two molecules, however the oscillator strength for Tookad is much lower compared with that of BPheid. Also for the low-lying excitations, Tookad provides lower oscillator strengths. This finding is partly supported by experiments as Pd-BChl displays a lower extinction coefficient for the higher energy bands compared to BPhe, albeit a higher extinction coefficient for the Q_y band.[3]

For comparison purposes, seven additional functionals, CAM-B3LYP, M06, M062X, ωB97X, ωB97, LC-ωPBE, and PBE0 (PBE1PBE) were included in the calculation of the excited states of Tookad and BPheid in toluene using the B3LYP geometry. The resulting spectra are shown in Figures 3 and 4, together with the previously obtained data for B3LYP, M06HF, and ωB97XD. The spectra display a significant difference between the funtionals, especially for the low-lying excitations. The Q_y band is clearly the strongest one, a feature common for all BChl's and an advantage when the compound is being used in PDT. The experimental absorption maxima of Tookad in toluene are positioned at 762, 535, 388, and 334 nm,[9] as also indicated in Figure 3. For BPheid there are, to our knowledge, no experimental spectroscopic data for the higher energy excitations in toluene, and only the two lowest-energy absorption maxima, at 758 and 531 nm,[4] are therefore indicated in Figure 4. From the spectra it can be concluded that ωB97XD displays the best positioned peak for the Q_y band for both Tookad and BPheid. The functional performance for the Tookad Q_y band is as follows: ωB97XD > CAM-B3LYP > M06-2X > M06 > M06HF > ωB97X > B3LYP > PBE1PBE > LC-ωPBE > ωB97. For BPheid the order is ωB97XD > M06HF > CAM-B3LYP > ωB97X > M06-2X > M06 > LC-ωPBE > ωB97 > B3LYP > PBE1PBE. For Bpheid, CAM-B3LYP and M06HF were equally close to the experimental value ($\Delta\lambda$ = 19 and 20 nm, respectively) but on opposite sides. The finding that CAM-B3LYP performs better than B3LYP on the lowest-lying excitation is supported by studies on Zn−bacteriochlorin and bacteriochlorin[55] as well as Zn−porphyrin in explicit aqueous solution,[56] in which the excitation energies are reduced when using CAM-B3LYP.
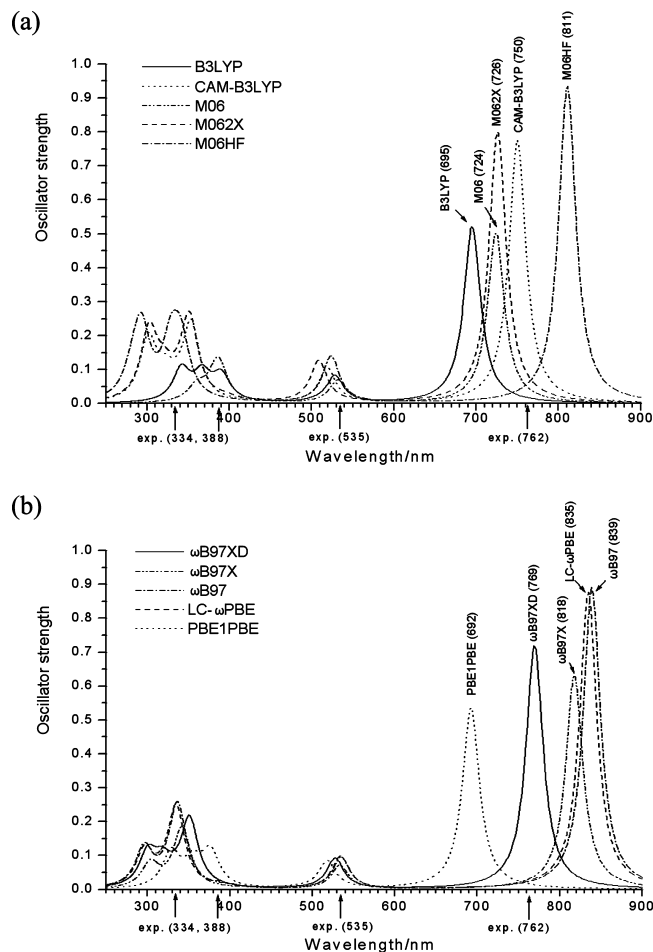
A Tookad Case Study

J. Chem. Theory Comput., Vol. 6, No. 7, 2010 **2091**

Figure 3. Absorption spectra of Tookad generated by (a) the B3LYP and M06 functional series and (b) the PBE and ωB97 functional series. Experimental values are displayed along the *x* axis.

LC-ωPBE and ωB97 generate absorptions at far too long wavelengths in both the case of Tookad and BPheid, meaning that the excitation energy is significantly underestimated. The opposite was observed for B3LYP and PBE1PBE that overestimated the excitation energy considerably (i.e., generating the absorption peak at far too short wavelength). B3LYP performs the best for the higher energy excitations of Tookad; however, this functional displays three peaks in the 300−400 nm region (also found when using THF as solvent), instead of two that are seen experimentally. The first and third peaks correspond very well to the experimental peaks found at 334 and 388 nm, whereas the second peak has no experimental match. The other functionals display two peaks each, albeit blue-shifted compared with B3LYP and experimental data. All functionals reproduce the small peak at 535 nm very well for Tookad, whereas for BPheid the functionals do not perform equally well in this case. Excitations with very small oscillator strengths, too small to be detected in the spectra, are generated by all functionals between the B and Q bands.

The effect of the basis sets (applied on all atoms but Pd) was investigated in the case of Tookad, and the resulting spectra obtained using the 6-31G(d,p), 6-31+G(d,p), and 6-311+G(2d,2p) basis sets are shown in Figure 5. The excited-state calculations were performed in toluene using
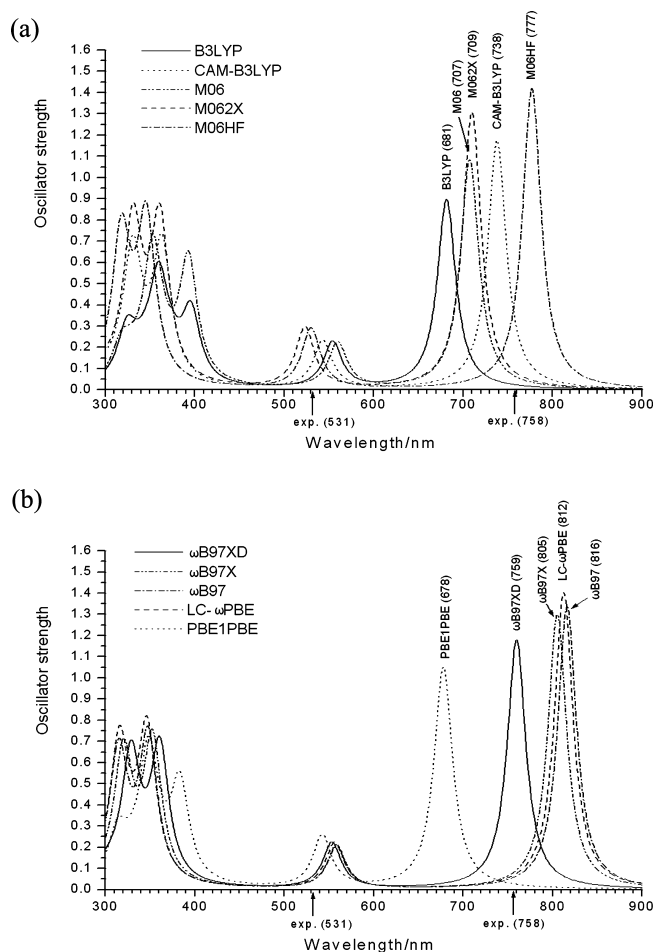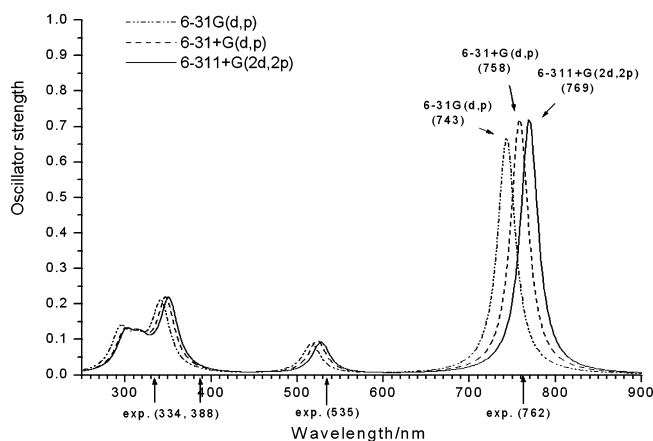

Figure 4. Absorption spectra of BPheid generated by (a) the B3LYP and M06 functional series and (b) the PBE and ωB97 functional series. Experimental values are displayed along the *x* axis.
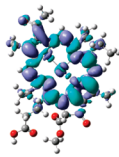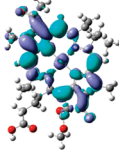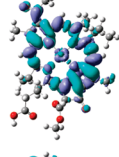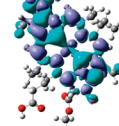

Figure 5. Absorption spectra for Tookad generated using ωB97XD in combination with three different basis sets. Experimental values are displayed along the *x* axis. Basis set for Pd is LanL2DZ throughout.

ωB97XD on the geometry generated at the B3LYP/6-31+G(d,p) level of theory. It can be seen that the larger basis sets with diffuse functions generate slightly better results, a difference that is seen mainly in the red-most region of the spectra. The basis set used in excited-state calculations has obviously a significantly smaller effect on the resulting

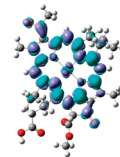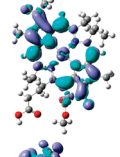**Table 3.** Electron Density Differences between the Ground and Excited States of Tookad Generated Using the ωB97XD Functional
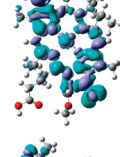
Excited state	Excitation energy/eV	Absorption/nm	Oscillator strength	Electron density difference between the ground state and excited state
1	1.6118	769	0.5396	
2	2.3503	528	0.1425	
9	3.5350	351	0.7192	
13	3.8974	318	0.1655	

Table 4. Electron Density Differences between the Ground and Excited States of Tookad Generated Using the B3LYP Functional
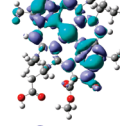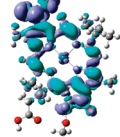
Excited state	Excitation energy/eV	Absorption/nm	Oscillator strength	Electron density difference between the ground state and excited state
1	1.7842	695	0.5220	
2	2.3473	528	0.1370	
8	3.1752	390	0.1397	
12	3.3815	367	0.1952	
14	3.6305	342	0.3930	

spectra than the functional, a conclusion that has also been found previously in the case of Zn−porphyrin.[29,30]

3.3. Electron Density Differences and Orbitals. As ωB97XD overall generated the most satisfying spectral results in this study, the computed electron density differences and orbitals of Tookad generated by this functional were investigated. For comparison the electron density differences and orbitals generated by B3LYP were also included. The 6-311+G(2d,2p) basis set was used together with toluene as the bulk solvent. The B3LYP geometry was used throughout. Electron density differences were calculated between the ground state and the excited states corresponding to the peaks displayed in the spectra. This means that four excited states were included for ωB97XD and five for B3LYP, as this functional generated an additional peak in the high-energy region of the spectra. The electron density differences for ωB97XD and B3LYP are displayed in Tables 3 and 4, respectively. Blue color represents a decrease in electron density and purple an increase in electron density of the excited state compared to the ground state. The density difference plots reveal that no dramatic restructuring of the electron distributions occur during the excitations; they are all essentially pure $\pi-\pi^*$ excitations within the aromatic cores. Albeit a minor shift in electron density can be noted between the different metal d-orbitals, only the fourth excitation displayed involves any considerable interaction between the aromatic core and the metal.

The HOMO-4 to LUMO+4 orbitals are displayed in the Supporting Information. In agreement with the electron density difference plots, the shapes of the orbitals generated by the two functionals are almost identical. The only minor differences in the shapes are seen for LUMO+2 and LUMO+1. In LUMO+2 the d_{z^2} orbital of Pd in B3LYP is replaced by a $d_{x^2-y^2}$ orbital in ωB97XD. In LUMO+1 the conjugated π orbital of the ring system using B3LYP has a considerably smaller extension than when using the ωB97XD functional. The two lowest excitations (corresponding to the Q_y and Q_x bands) occur between HOMO and LUMO and between HOMO-1 and LUMO, respectively, for all functionals and for both Tookad and BPheid. However, as clearly seen in the absorption spectra, the excitation energies are obviously different. The energy gap between HOMO and LUMO is smaller when using ωB97XD compared with the same energy gap for B3LYP, which is also reflected in that ωB97XD overall generates the Q_y band at longer wavelengths than B3LYP. The higher energy excitations (the B bands) do not occur between the same orbitals for the different functionals, and those excitations involve more than only the two highest occupied and the two lowest unoccupied molecular orbitals, indicating that the four-orbital model does not correctly describe these transitions.

4. Conclusions

Tookad is a Pd-coordinated bacteriopheophorbide (Pd-BPheid) that has shown promising photodynamic properties, especially on prostate tumors. The low-lying excitations of Tookad and metal-free BPheid were studied computationally with the aim to reproduce the long-wavelength region of the absorption spectra through the use of time-dependent density functional theory (TD-DFT) in combination with new range-separated and meta hybrid density functional theory (DFT)

A Tookad Case Study

J. Chem. Theory Comput., Vol. 6, No. 7, 2010 **2093**

functionals. The commonly employed B3LYP functional was also included in the study, as it is well-known that this functional overestimates excitation energies.

B3LYP, M06HF, and ωB97XD were used for excited-state calculations on Tookad and BPheid geometries generated at the B3LYP and M06 level of theory, respectively, in toluene and tetrahydrofuran (THF). No significant difference was found in the calculated absorption spectra by the use of either B3LYP or M06 in geometry optimizations. For the excited-state calculations, ωB97XD was found to generate the Q_y transition band (the red-most absorption) closest to the experimental position, for both Tookad and BPheid. However, for the Q_x band (the second red-most absorption) the results are more inconsistent, with either B3LYP or ωB97XD generating the best results for Tookad and M06HF generating the best results for BPheid. In the case of Tookad, the three functionals do however perform highly equal for the Q_x band. When the CAM-B3LYP, M06, M06-2X, ωB97X, ωB97, LC-ωPBE, and PBE0 (PBE1PBE) functionals are included in the excited-state calculations of Tookad and BPheid in toluene, ωB97XD still performs the best for the Q_y band, followed by CAM-B3LYP. LC-ωPBE and ωB97 underestimate and B3LYP and PBE0 overestimate the Q_y band excitation energy considerably. These data hence differ from earlier benchmarking work, in which PBE0 was of consistently reasonable quality. A set of calculations with three different basis sets, with and without diffuse functions, indicated that the basis set has a minor effect on the calculated spectra. The overall accuracy for the Q_y band was 0–0.02 and 0–0.05 eV for Tookad and BPheid, respectively, for the ωB97XD functional.

We emphasize that the study is conducted on a limited system and that further work is needed in order to find the optimal combination of functionals and basis sets for optimizations and excitations. Clear from the current study is, however, that the evaluation of low-lying excitations is less straightforward to obtain at high accuracy than those in the UV region of the spectrum and that functionals that from a rational perspective cannot be justified for the current property seem to perform surprisingly well whereas others developed particularly with valence excitations in mind do not. It is also concluded that, whereas statistical treatment on a very large set of structurally divergent molecules may favor certain functionals, when focusing in on a particular class of compounds or a specific wavelength range, the results may be entirely different.

Supporting Information Available: Cartesian coordinates for geometries of Tookad optimized in gas phase, THF and toluene using B3LYP and M06 functionals. This material is available free of charge via the Internet at http://pubs.acs.org.

References

(1) Henderson, B. W.; Sumlin, A. B.; Owczarczak, B. L.; Dougherty, T. J. *J. Photochem. Photobiol., B* **1991**, *10*, 303–313.

(2) Dougherty, T. J. Bacteriochlorophyll-A derivatives useful in photodynamic therapy. U.S. Patent 5,171,741, Dec 15, 1992.

(3) Hartwich, G.; Fiedor, L.; Simonin, I.; Cmiel, E.; Schafer, W.; Noy, D.; Scherz, A.; Scheer, H. *J. Am. Chem. Soc.* **1998**, *120*, 3675–3683.

(4) Limantara, L.; Sakamoto, S.; Koyama, Y.; Nagae, H. *Photochem. Photobiol.* **1997**, *65*, 330–337.

(5) Noy, D.; Fiedor, L.; Hartwich, G.; Scheer, H.; Scherz, A. *J. Am. Chem. Soc.* **1998**, *120*, 3684–3693.

(6) Geskes, C.; Hartwich, G.; Scheer, H.; Mantele, W.; Heinze, J. *J. Am. Chem. Soc.* **1995**, *117*, 7776–7783.

(7) Sundholm, D. *Chem. Phys. Lett.* **1999**, *302*, 480–484.

(8) Sundholm, D. *Chem. Phys. Lett.* **2000**, *317*, 545–552.

(9) Musewald, C.; Hartwich, G.; Pollinger-Dammer, F.; Lossau, H.; Scheer, H.; Michel-Beyerle, M. E. *J. Phys. Chem.* **1998**, *102*, 8336–8342.

(10) Vakrat-Haglili, Y.; Weiner, L.; Brumfeld, V.; Brandis, A.; Salomon, Y.; McIlroy, B.; Wilson, B. C.; Pawlak, A.; Rozanowska, M.; Sarna, T.; Scherz, A. *J. Am. Chem. Soc.* **2005**, *127*, 6487–6497.

(11) Scherz, A.; Salomon, Y.; Brandis, A.; Scheer, H.; Palladium-substituted bacteriochlorophyll derivatives and use thereof. U.S. Patent 6,569,846, May 27, 2003.

(12) Chen, Q.; Huang, Z.; Luck, D.; Beckers, J.; Brun, P. H.; Wilson, B. C.; Scherz, A.; Salomon, Y.; Hetzel, F. W. *Photochem. Photobiol.* **2002**, *76*, 438–445.

(13) Schreiber, S.; Gross, S.; Brandis, A.; Harmelin, A.; Rosenbach-Belkin, V.; Scherz, A.; Salomon, Y. *Int. J. Cancer* **2002**, *99*, 279–285.

(14) Koudinova, N. V.; Pinthus, J. H.; Brandis, A.; Brenner, O.; Bendel, P.; Ramon, J.; Eshhar, Z.; Scherz, A.; Salomon, Y. *Int. J. Cancer* **2003**, *104*, 782–789.

(15) Borle, F.; Radu, A.; Fontolliet, C.; van den Bergh, H.; Monnier, P.; Wagnieres, G. *Br. J. Cancer* **2003**, *89*, 2320–2326.

(16) Borle, F.; Radu, A.; Monnier, P.; van den Bergh, H.; Wagnieres, G. *Photochem. Photobiol.* **2003**, *78*, 377–383.

(17) Preise, D.; Mazor, O.; Koudinova, N.; Liscovitch, M.; Scherz, A.; Salomon, Y. *Neoplasia* **2003**, *5*, 475–480.

(18) Trachtenberg, J.; Bogaards, A.; Weersink, R. A.; Haider, M. A.; Evans, A.; McCluskey, S. A.; Scherz, A.; Gertner, M. R.; Yue, C.; Appu, S.; Aprikian, A.; Savard, J.; Wilson, B. C.; Elhilali, M. *J. Urol.* **2007**, *178*, 1974–1979.

(19) Haider, M. A.; Davidson, S. R. H.; Kale, A. V.; Weersink, R. A.; Evans, A. J.; Toi, A.; Gertner, M. R.; Bogaards, A.; Wilson, B. C.; Chin, J. L.; Elhilali, M.; Trachtenberg, J. *Radiology* **2007**, *244*, 196–204.

(20) Weersink, R. A.; Forbes, J.; Bisland, S.; Trachtenberg, J.; Elhilali, M.; Brun, P. H.; Wilson, B. C. *Photochem. Photobiol.* **2005**, *81*, 106–113.

(21) Trachtenberg, J.; Weersink, R. A.; Davidson, S. R. H.; Haider, M. A.; Bogaards, A.; Gertner, M. R.; Evans, A.; Scherz, A.; Savard, J.; Chin, J. L.; Wilson, B. C.; Elhilali, M. *BJU Int.* **2008**, *102*, 556–562.

(22) Brun, P. H.; DeGroot, J. L.; Dickson, E. F. G.; Farahani, M.; Pottier, R. H. *Photochem. Photobiol. Sci.* **2004**, *3*, 1006–1010.

(23) Tozer, D. J.; Amos, R. D.; Handy, N. C.; Roos, B. O.; Serrano-Andres, L. *Mol. Phys.* **1999**, *97*, 859–868.

(24) Perpète, E. A.; Wathelet, V.; Preat, J.; Lambert, C.; Jacquemin, D. *J. Chem. Theory Comput.* **2006**, *2*, 434–440.

(25) Andzelm, J.; Rinderspacher, B. C.; Rawlett, A.; Dougherty, J.; Baer, R.; Govind, N. *J. Chem. Theory Comput.* **2009**, *5*, 2835–2846.

(26) Jacquemin, D.; Wathelet, V.; Perpète, E. A.; Adamo, C. *J. Chem. Theory Comput.* **2009**, *5*, 2420–2435.

(27) Jacquemin, D.; Perpète, E. A.; Ciofini, I.; Adamo, C. *J. Chem. Theory Comput.* **2010**, *6*, 1532–1537.

(28) Palma, M.; Cardenas-Jiron, G. I.; Rodriguez, M. I. M. *J. Phys. Chem. A* **2008**, *112*, 13574–13583.

(29) Nguyen, K. A.; Day, P. N.; Pachter, R. *J. Chem. Phys.* **1999**, *110*, 9135–9144.

(30) Nguyen, K. A.; Pachter, R. *J. Chem. Phys.* **2001**, *114*, 10757–10767.

(31) Gouterman, M. *J. Mol. Spectrosc.* **1961**, *6*, 138–163.

(32) Houssier, C.; Sauer, K. *J. Am. Chem. Soc.* **1970**, *92*, 779–791.

(33) Fragata, M.; Norden, B.; Kurucsev, T. *Photochem. Photobiol.* **1988**, *47*, 133–143.

(34) Hasegawa, J.; Ozeki, Y.; Ohkawa, K.; Hada, M.; Nakatsuji, H. *J. Phys. Chem. B* **1998**, *102*, 1320–1326.

(35) Parusel, A. B. J.; Grimme, S. *J. Phys. Chem. B* **2000**, *104*, 5395–5398.

(36) Becke, A. D. *J. Chem. Phys.* **1993**, *98*, 5648–5652.

(37) Adamo, C.; Barone, V. *J. Chem. Phys.* **1999**, *110*, 6158–6170.

(38) Tawada, Y.; Tsuneda, T.; Yanagisawa, S.; Yanai, T.; Hirao, K. *J. Chem. Phys.* **2004**, *120*, 8425–8433.

(39) Vydrov, O. A.; Scuseria, G. E. *J. Chem. Phys.* **2006**, *125*, 234109.

(40) Vydrov, O. A.; Heyd, J.; Krukau, A. V.; Scuseria, G. E. *J. Chem. Phys.* **2006**, *125*, 074106.

(41) Vydrov, O. A.; Scuseria, G. E.; Perdew, J. P. *J. Chem. Phys.* **2007**, *126*, 154109.

(42) Yanai, T.; Tew, D. P.; Handy, N. C. *Chem. Phys. Lett.* **2004**, *393*, 51–57.

(43) Chai, J. D.; Head-Gordon, M. *J. Chem. Phys.* **2008**, *128*, 084–106.

(44) Chai, J. D.; Head-Gordon, M. *Phys. Chem. Chem. Phys.* **2008**, *10*, 6615–6620.

(45) Zhao, Y.; Truhlar, D. G. *Theor. Chem. Acc.* **2007**, *120*, 215–241.

(46) Zhao, Y.; Truhlar, D. G. *J. Phys. Chem.* **2006**, *110*, 5121–5129.

(47) Zhao, Y.; Truhlar, D. G. *J. Phys. Chem.* **2006**, *110*, 13126–13130.

(48) Frisch, M. J.; Trucks, G. W.; Schlegel, H. B.; Scuseria, G. E.; Robb, M. A.; Cheeseman, J. R.; Scalmani, G.; Barone, V.; Mennucci, B.; Petersson, G. A.; Nakatsuji, H.; Caricato, M.; Li, X.; Hratchian, H. P.; Izmaylov, A. F.; Bloino, J.; Zheng, G.; Sonnenberg, J. L.; Hada, M.; Ehara, M.; Toyota, K.; Fukuda, R.; Hasegawa, J.; Ishida, M.; Nakajima, T.; Honda, Y.; Kitao, O.; Nakai, H.; Vreven, T.; Montgomery, J. A., Jr.; Peralta, J. E.; Ogliaro, F.; Bearpark, M.; Heyd, J. J.; Brothers, E.; Kudin, K. N.; Staroverov, V. N.; Kobayashi, R.; Normand, J.; Raghavachari, K.; Rendell, A.; Burant, J. C.; Iyengar, S. S.; Tomasi, J.; Cossi, M.; Rega, N.; Millam, J. M.; Klene, M.; Knox, J. E.; Cross, J. B.; Bakken, V.; Adamo, C.; Jaramillo, J.; Gomperts, R.; Stratmann, R. E.; Yazyev, O.; Austin, A. J.; Cammi, R.; Pomelli, C.; Ochterski, J. W.; Martin, R. L.; Morokuma, K.; Zakrzewski, V. G.; Voth, G. A.; Salvador, P.; Dannenberg, J. J.; Dapprich, S.; Daniels, A. D.; Farkas, O.; Foresman, J. B.; Ortiz, J. V.; Cioslowski, J.; Fox, D. J. *Gaussian09*, Revision A.02; Gaussian, Inc.: Wallingford, CT, 2009.

(49) Hay, P. J.; Wadt, W. R. *J. Chem. Phys.* **1985**, *82*, 270–283.

(50) Mennucci, B.; Cammi, R.; Tomasi, J. *J. Chem. Phys.* **1998**, *109*, 2798–2807.

(51) Chipman, D. M. *J. Chem. Phys.* **2000**, *112*, 5558–5565.

(52) Casida, M. E. In *Recent Advances in Density Functional Methods, Part 1*; Chong, D. P., Ed.; World Scientific: Singapore, 1995; p 155−192.

(53) Stratmann, R. E.; Scuseria, G. E.; Frisch, M. J. *J. Chem. Phys.* **1998**, *109*, 8218–8224.

(54) Casida, M. E.; Jamorski, C.; Casida, K. C.; Salahub, D. R. *J. Chem. Phys.* **1998**, *108*, 4439–4449.

(55) Kobayashi, R.; Amos, R. D. *Chem. Phys. Lett.* **2006**, *420*, 106–109.

(56) Govind, N.; Valiev, M.; Jensen, L.; Kowalski, K. *J. Phys. Chem. A* **2009**, *113*, 6041–6043.